

SLAVKO BERNIK^{1*}, MATEJA KOŠIR^{1,2},
EMMANUEL GUILMEAU³

¹Jožef Stefan Institute, Ljubljana, Slovenia, ²Jožef Stefan
International Postgraduate School, Ljubljana, Slovenia,

³Laboratoire CRISMAT, UMR 6508 CNRS/ENSICAEN, CAEN
Cedex, France

Scientific paper

ISSN 0351-9465, E-ISSN 2466-2585

UDC: 620.179:620.193.94

doi:10.5937/ZasMat1602318B



Zastita Materijala 57 (2)

318 - 325 (2016)

Microstructure and thermoelectric characteristics of $(\text{ZnO})_k\text{In}_2\text{O}_3$ - based ceramics ($k = 5$ and 11)

ABSTRACT

Oxide thermoelectric ceramics are needed for high-temperature applications that involve harvesting the waste heat by direct transformation into electricity. In the case of *n*-type materials, the homologous $(\text{ZnO})_k\text{In}_2\text{O}_3$ -type phases are very promising for tailoring the TE properties. In this investigation the thermoelectric $(\text{ZnO})_k\text{In}_2\text{O}_3$ -based ceramics for $k=5$ and 11 were prepared using a classic ceramics procedure and sintering at $1500\text{ }^\circ\text{C}$. During their preparation, either a fresh powder mixture of ZnO and In_2O_3 or a mixture of ZnO and In_2O_3 also containing plate-like grains of the pre-reacted $(\text{ZnO})_k\text{In}_2\text{O}_3$ phases was used to induce possible microstructure texturing. It was demonstrated that the starting composition in terms of k value and the type of starting powder mixture affect the processes, leading to the formation of the equilibrium $(\text{ZnO})_k\text{In}_2\text{O}_3$ homologous phase and, consequently, also the microstructure development. Nevertheless, all the samples had similar final microstructures and no texturing was observed. Regardless of the use of different starting-powder mixtures, the samples with the same composition had a similar ZT: at 627°C it was 0.11 for the samples with $k=5$ and 0.08 for $k=11$, which is not so inferior if we take account of the significantly lower content of In_2O_3 in these samples.

Keywords: ZnO ceramics, In_2O_3 doping, microstructure, thermoelectric characteristics.

1. INTRODUCTION

Thermoelectric (TE) materials are characterized by the thermoelectric effect, which actually includes three separate effects: the Seebeck effect, the Peltier effect, and the Thomson effect. Cooling devices based on the Peltier effect, made from classic TE alloys, are already well established in various high technologies. The exploitation of another characteristic of TE materials, the Seebeck effect, nowadays represents one of the key technological challenges, as modules made from *n*- and *p*-type TE materials give the only viable possibility for harvesting waste heat by its direct conversion into electricity. The effective utilization of the waste heat, which represents almost 70% of all primary produced energy, could be an important pillar of energy sustainability [1-5]

*Corresponding author: Slavko Bernik

E-mail: slavko.bernik@ijs.si

Paper received: 09. 03. 2016.

Paper accepted: 14. 04. 2016.

Paper is available on the website:

www.idk.org.rs/journal

The thermoelectric (TE) characteristics of materials are usually expressed by the dimensionless figure of merit ZT, in accordance with the equation $ZT = S^2\sigma T/\kappa$, where S is the Seebeck coefficient, σ is the electrical conductivity and κ is the thermal conductivity. For good TE characteristics a reasonably good electrical conductivity, a high Seebeck coefficient and a low thermal conductivity of the material are required, which demands an intricate optimization of juxtaposed parameters. The best TE materials, i.e., metallic alloys, already have the required thermoelectric characteristics, with ZT values of approximately 2. However, they are thermally unstable in air at temperatures above $300\text{ }^\circ\text{C}$ and are made from expensive and toxic elements.[2,6,7] Their limitations suggest the potential advantages of oxide TE materials at higher temperatures: they are thermally and chemically stable in oxygen to at least 800°C , non-toxic and made from abundantly available and low-cost elements. However, these advantages can only be realized after a significant improvement of their TE characteristics, which are for polycrystalline ceramics much too low, with ZT values mostly well below 1 [8-10].

Oxide thermoelectric materials came into focus in 1997 with the report of Terasaki et al. [11] that the transition-metal oxide NaCo_2O_4 exhibits a large thermos-power and a low electrical resistivity. While NaCo_2O_4 is known to be highly unstable, due to its poor resistance to humidity and its volatility at elevated temperatures, other p-type Co-based oxides with a misfit layered structure, such as $\text{Ca}_3\text{Co}_4\text{O}_9$ and $\text{Bi}_2\text{Sr}_2\text{Co}_2\text{O}_y$, are much better in this regard and at the same time also very promising for further enhancements of the TE properties [9,10]. The properties of all these materials are closely related to their complex structure. In the case of $\text{Ca}_3\text{Co}_4\text{O}_9$ the structure consists of a CoO_2 layer of the CdI_2 type, ensuring an electrically conductive and an insulating Ca_2CoO_3 layer of the rock-salt type. The mismatch and the weak connection between these two substructure types contribute to the phonon scattering for a reduced thermal conductivity. Hence, the $\text{Ca}_3\text{Co}_4\text{O}_9$ has a noticeably higher electrical conductivity in the a-b (in-plane) direction along the CoO_2 layers than in the c (out-of-plane) direction with a lower thermal conductivity. The $\text{Ca}_3\text{Co}_4\text{O}_9$ phase also has a distinct plate-like morphology of the grains. Generally, a high density and texturing are considered as the main microstructural features for an improvement in the thermoelectric characteristics of materials with anisotropic properties, such as $\text{Ca}_3\text{Co}_4\text{O}_9$ ceramics. Our research showed the limitations of such an approach; for a completely random orientation of plate-like grains and densities below 60% the $\text{Ca}_3\text{Co}_4\text{O}_9$ ceramics had a ZT of 0.09 at 627 °C, while in perfectly textured and fully dense (99%) samples the ZT was 0.17. The highest ZT of 31 was obtained in modestly textured, but still highly porous, ceramics having a similar electrical conductivity and Seebeck coefficient in comparison to the perfectly textured ceramics, although with a much lower thermal conductivity [12]. To the best of our knowledge this is the highest ZT value reported so far for undoped $\text{Ca}_3\text{Co}_4\text{O}_9$ ceramics.

The n-type TE materials in the focus of our research are SrTiO_3 , CaMnO_3 and ZnO. They have a large Seebeck coefficient; however, for a higher ZT the low electrical and the high thermal conductivity should be significantly improved by proper doping and microstructure optimisation [9]. The undoped polycrystalline ZnO ceramics have a too low electrical conductivity of about 10S/cm and a too high thermal conductivity of about 40W/mK for good thermoelectric characteristics, despite the very high Seebeck coefficient of about $-400\mu\text{V/K}$. [8] However, proper doping of the ZnO ceramics with either Al [13] or a combination of Al and Ga [14] resulted in the best ZT values for the n-type polycrystalline ceramics up to about 0.65 at 700 °C. A very interesting basis for the tailoring of the TE

properties is offered by doping with In_2O_3 , introducing multiple complex planar defects into the relatively simple ZnO wurtzite-type structure and consequently the formation of homologous $(\text{ZnO})_k\text{In}_2\text{O}_3$ -type phases at temperatures above 1100 °C [15]. Basically, two types of defects are formed that primarily affect the TE characteristics: planar InO_2 defects along the (0001)-basal planes as highly electron-conductive pathways and “zig-zag”-type ZnO/In defects in between the planar ones, causing phonon scattering for a reduced thermal conductivity. The homologous $(\text{ZnO})_k\text{In}_2\text{O}_3$ phases are defined by the distance between the planar InO_2 defects in accordance with the expression $d = k+1$, where d is the number of the ZnO layers. The TE characteristics of $(\text{ZnO})_k\text{In}_2\text{O}_3$ -based ceramics were studied for compositions with $k=3,5,7$ and 9, and so far the highest ZT of about 0.1 at 700 °C was based on $(\text{ZnO})_5\text{In}_2\text{O}_3$. [16-18] The planar defects and hence the homologous $(\text{ZnO})_k\text{In}_2\text{O}_3$ phases form through the mechanism of internal diffusion; this is driven by a local charge deficiency, initiated by the Zn vacancies as preferential sites for the incorporation of the In^{3+} ions into the wurtzite structure of ZnO [19]. The formation of the planar defects also strongly influences the grain growth and the grains of the $(\text{ZnO})_k\text{In}_2\text{O}_3$ homologous phases develop a plate-like morphology, which gives the possibility of tailoring a textured microstructure. In highly textured $(\text{ZnO})_5\text{In}_2\text{O}_3$ ceramics the ZT value was increased to 0.18 at 800 °C. [20] This again confirmed the importance of a microstructure optimisation for the improvement of the TE characteristics of ceramics in the ZnO- In_2O_3 system.

In this work the $(\text{ZnO})_k\text{In}_2\text{O}_3$ -based ceramics for $k=5$ and 11 were prepared using a classic ceramics procedure and sintering at 1500 °C. The samples were prepared either from a fresh powder mixture of ZnO and In_2O_3 or from a mixture of ZnO and In_2O_3 with the addition of a pre-reacted powder with well-defined plate-like grains of the $(\text{ZnO})_k\text{In}_2\text{O}_3$ homologous phases for possible microstructure texturing. The influence of the composition in terms of k value and the starting powder mixture on the phase formation, the grain growth and the microstructure development, and consequently the TE characteristics of the $(\text{ZnO})_k\text{In}_2\text{O}_3$ -based ceramics, was studied.

2. EXPERIMENTAL

Powder mixtures with compositions $(\text{ZnO})_k\text{In}_2\text{O}_3$ for k values of 5 and 11 were prepared from powders of ZnO (Grillo Zinkoxide, GmbH, Pharma 4, > 99.9%) and In_2O_3 (Alfa Aesar, 99.9 % metals basis, 325 mesh powder), mixed with ethanol and homogenized in a polyethylene vial in a planetary ball mill for 1 h, and

afterwards dried at 80 °C (fresh powder mixtures labeled Zkl). Part of each powder mixture Zkl was in a loose state pre-reacted at 1150 °C for 2 hours and subsequently grinded in an agate mortar. The pre-reacted powder of each composition k was mixed with a corresponding fresh powder mixture Zkl of ZnO and In_2O_3 in the weight ratio 1:1 and homogenized in an agate mortar (powder mixtures labeled Zkl 50-50). The powder mixtures, fresh (Zkl) and those containing pre-reacted powder (Zkl 50-50) were uniaxially pressed into pellets with a diameter of 12 mm and height of approximately 2 mm, followed by cold isostatic pressing under a pressure of 280 MPa with a 30 s holding time. The pellets were sintered at 1500 °C for 2 hours in air. The density of the samples was measured using Archimedes' principle (DENSITEC). The phase composition of the sintered samples was analyzed using powder X-ray diffraction analysis (diffractometer PANalytical X'Pert PRO MPD, Almelo, The Netherlands). The microstructures in the cross-section direction across the disc samples, un-etched and thermally etched, were examined using a scanning electron microscope (SEM, JSM-5800, JEOL, Tokyo, Japan) equipped with an energy-dispersive X-ray spectrometer (EDS; Link ISIS 300, Oxford Instruments Ltd., Oxfordshire, U.K.). Rods with lengths from 8 to 10 mm and a cross-section of about $2 \times 2 \text{ mm}^2$ were cut from the sintered pellets for measurements of the Seebeck coefficient and the electrical conductivity using a commercial ZEM 3 device (ULVAC Technologies, Inc, Methuen, MA, USA) in a partial helium atmosphere. For the thermal diffusivity measurements, squares of $6 \times 6 \text{ mm}^2$ and 1 mm thick were cut from the pellet and measured in air with a laser flash (NETZSCH, LFA 457 MicroFlash, Netzsch, GmbH, Germany) without any additional carbon coating. The thermal conductivity was calculated from the heat capacity (C_p), density (ρ) and thermal diffusivity (α), according to the formula:

$$\kappa = C_p * \rho * \alpha$$

3. RESULTS AND DISCUSSION

The XRD patterns of the loose powder mixtures pre-reacted at 1150 °C are presented in Fig. 1. Only in the powder mixture for $k=5$ with the highest amount of In_2O_3 added to the ZnO was the homologous phase of the starting composition $\text{Zn}_5\text{In}_2\text{O}_8$ (JC PDF 00-020-1440) formed. In the powder mixtures Z111 the $\text{Zn}_5\text{In}_2\text{O}_8$ and $\text{Zn}_7\text{In}_2\text{O}_{10}$ (JC PDF 00-020-1441) homologous phases were clearly detected, while the XRD pattern also indicates the possible formation of the phases for $k \geq 11$ towards the pure ZnO phase, which could be identified in accordance with the report of Moriga et al. [15] They also reported that only $(\text{ZnO})_5\text{In}_2\text{O}_3$

and $(\text{ZnO})_7\text{In}_2\text{O}_3$ are stable at 1100 °C. Nevertheless, such a complete formation of the $(\text{ZnO})_5\text{In}_2\text{O}_3$ phase at 1150 °C was in a way surprising, having in mind the likely relatively weak contact between the reacting ZnO and In_2O_3 in the pre-reacted loose powder mixture Z5I. It was also demonstrated in the well-defined, plate-like morphology of the several-micrometer-sized grains (Fig. 2), with the largest having a length up to $5 \mu\text{m}$ and a thickness of approximately $0.8 \mu\text{m}$. Poor homogeneity in the distribution of the In_2O_3 in the ZnO should also be taken into consideration, especially for the compositions with a higher k and small additions of In_2O_3 , even more so because the ZnO powder is much finer than the In_2O_3 (Fig. 2). In the case of Z5I the addition of In_2O_3 to ZnO was obviously sufficient to ensure its presence everywhere in the pre-reacted mixture in an amount needed for the relatively uniform formation of the $(\text{ZnO})_5\text{In}_2\text{O}_3$ phase. However, in the Z111 a much smaller amount of In_2O_3 is likely to be un-homogeneously distributed; locally it could be, with respect to the nominal starting composition, either in excess or deficit with respect to the ZnO, which allowed, on the one hand, the formation of the $(\text{ZnO})_5\text{In}_2\text{O}_3$ and $(\text{ZnO})_7\text{In}_2\text{O}_3$ phases, and on the other hand, the formation of higher k homologous phases towards the pure ZnO, respectively.

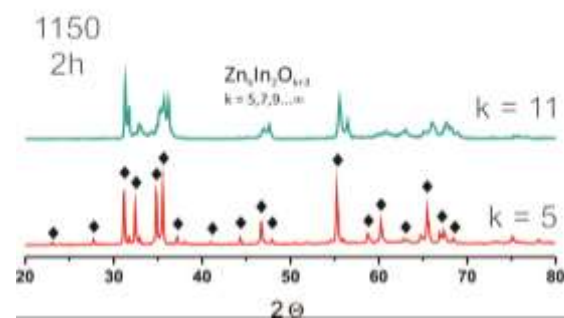
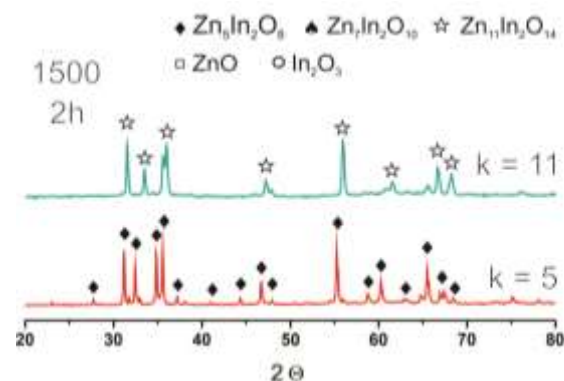


Figure 1 - The XRD patterns of powder mixtures pre-reacted at 1150 °C and the samples sintered at 1500 °C.

length up to $5\mu\text{m}$ and a thickness of approximately $0.8\mu\text{m}$. Poor homogeneity in the distribution of the In_2O_3 in the ZnO should also be taken into consideration, especially for the compositions with a higher k and small additions of In_2O_3 , even more so because the ZnO powder is much finer than the In_2O_3 (Fig. 2). In the case of Z5I the addition of In_2O_3 to ZnO was obviously sufficient to ensure its presence everywhere in the pre-reacted mixture in an amount needed for the relatively uniform

formation of the $(\text{ZnO})_5\text{In}_2\text{O}_3$ phase. However, in the Z11I a much smaller amount of In_2O_3 is likely to be un-homogeneously distributed; locally it could be, with respect to the nominal starting composition, either in excess or deficit with respect to the ZnO, which allowed, on the one hand, the formation of the $(\text{ZnO})_5\text{In}_2\text{O}_3$ and $(\text{ZnO})_7\text{In}_2\text{O}_3$ phases, and on the other hand, the formation of higher k homologous phases towards the pure ZnO, respectively.

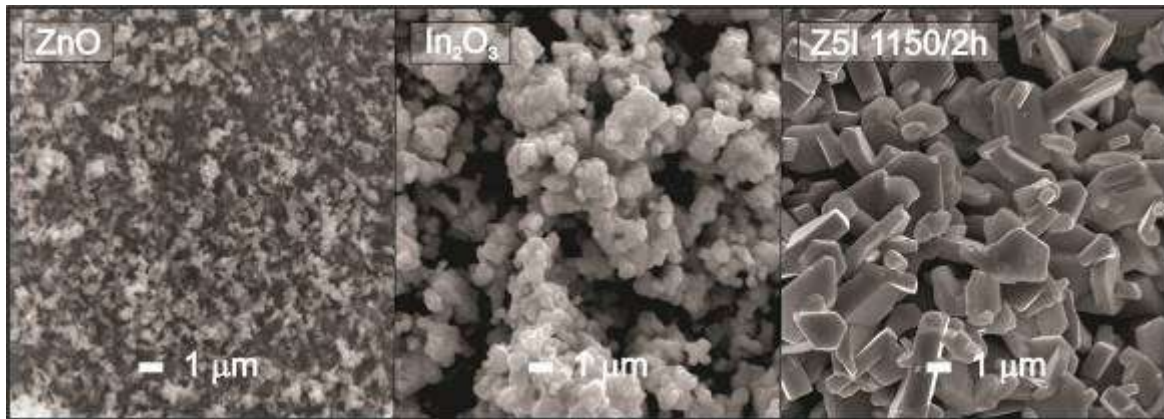


Figure 2 - SEM images of the starting ZnO and In_2O_3 powders, and the powder with composition $(\text{ZnO})_5\text{In}_2\text{O}_3$ pre-reacted in loose form at 1150°C

In comparison to the pre-reacted powder Z5I from essentially only the $(\text{ZnO})_5\text{In}_2\text{O}_3$ phase, the pre-reacted powder of Z11I has a much more complex phase composition containing some $(\text{ZnO})_5\text{In}_2\text{O}_3$ and $(\text{ZnO})_7\text{In}_2\text{O}_3$, and a significant share of phases for $k \geq 11$, towards the practically pure ZnO phase. Nevertheless, it also has a similar well-expressed, plate-like morphology of the grains. The addition of such pre-reacted powders of Z5I and Z11I with much larger grains and a well-defined, plate-like morphology to the corresponding fresh mixtures of ZnO and In_2O_3 with a much finer grain size (Fig. 2) could strongly affect the microstructure development of the ZkI 50-50 samples. In accordance with Ostwald ripening, the preferential growth of the larger grains of the pre-reacted powders could be expected with the possible development of at least a certain degree of microstructure texturing due to the plate-like morphology.

The pellets prepared from the powder mixtures ZkI and ZkI 50-50 ($k=5,11$) were sintered at 1500°C . At such a high sintering temperature the rapid development of the homologous phases corresponding to the starting compositions, the $(\text{ZnO})_5\text{In}_2\text{O}_3$ in the Z5I and Z5I 50-50 samples, and the $(\text{ZnO})_{11}\text{In}_2\text{O}_3$ in the Z11I and Z11I 50-50 samples, could be expected. At temperatures above 1300°C a significant sublimation of the ZnO

takes place, as reported by Anthrop and Searcy [21], which results in the increased formation of Zn vacancies. An abundance of Zn vacancies enhances the self-diffusion of the Zn. They are also preferential sites for the incorporation of In^{3+} and its diffusion into the ZnO, which leads to the formation of multiple planar defects and hence homologous phases in accordance with the mechanism of internal diffusion [19]. Accordingly, the XRD analysis clearly showed that all the samples sintered at 1500°C for 2 hours have the composition of an equilibrium homologous phase for the starting k value, the $\text{Zn}_5\text{In}_2\text{O}_8$ or the $\text{Zn}_{11}\text{In}_2\text{O}_{14}$.

The microstructures of the samples sintered at 1500°C are presented in Fig. 3. All the samples have a relatively homogeneous microstructure with randomly oriented, plate-like grains. The sample Z5I prepared from a fresh powder mixture of ZnO and In_2O_3 has a smaller grain size than the other samples, especially in comparison to the sample Z11I, also prepared from a fresh powder mixture.

Such a microstructure development can be explained in terms of the distribution of the In_2O_3 in the powder mixture with ZnO and its local concentrations regarding the In_2O_3 -to-ZnO ratio; it controls the phase formation, as was already shown in the case of powders pre-reacted at 1150°C , and via phase formation consequently also the grain growth.

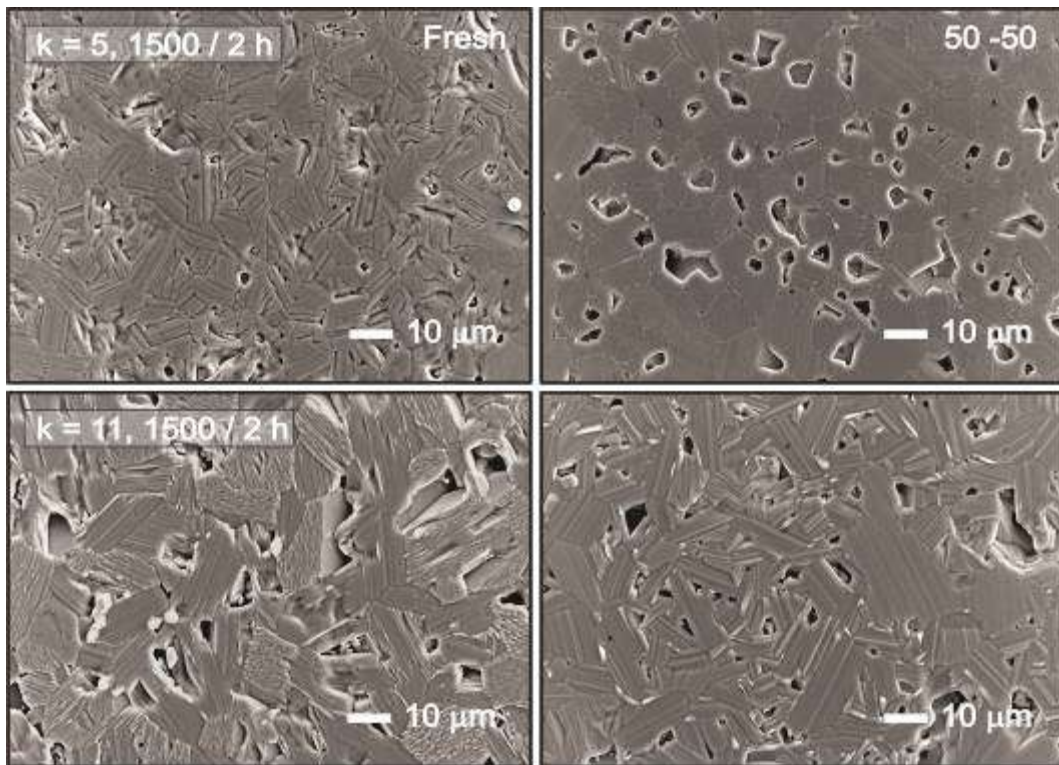


Figure 3 - Thermally etched microstructures of the $(\text{ZnO})_k\text{In}_2\text{O}_3$ ($k=5,11$) ceramics, prepared from the fresh powder mixtures of ZnO and In_2O_3 (fresh) or starting mixture containing also pre-reacted powder (50-50), sintered at 1500°C for 2 hours.

In the Z5I sample the amount of In_2O_3 is sufficient to ensure that everywhere in the powder mixture at short range the In_2O_3 -to-ZnO ratio is close to 5, which enables the formation of the $(\text{ZnO})_5\text{In}_2\text{O}_3$ homologous phase uniformly through the sample and hence uniform grain growth with a finer grain size. For a much smaller amount than in the sample Z11I the coarse-grained In_2O_3 is distributed inhomogeneously in much finer ZnO, locally being either in excess (i.e., In_2O_3 -to-ZnO ratio < 11) or in deficit (i.e., In_2O_3 -to-ZnO > 11). As in the powder Z11I pre-reacted at 1150°C , also in the sample sintered at 1500°C (however at a much faster rate) grains of the $(\text{ZnO})_5\text{In}_2\text{O}_3$ and $(\text{ZnO})_7\text{In}_2\text{O}_3$ phases are initially formed at the In_2O_3 -rich locations. They are separated by grains of phases $(\text{ZnO})_k\text{In}_2\text{O}_3$ with $k > 11$ going towards the pure ZnO, which are formed in areas with a deficit of In_2O_3 . As the growth of the grains is dictated by the formation of planar defects with the diffusion of In_2O_3 into the ZnO, the grains of $(\text{ZnO})_5\text{In}_2\text{O}_3$ and $(\text{ZnO})_7\text{In}_2\text{O}_3$ with a larger concentration of defects are likely to be larger from the very beginning than the grains of the high- k phases. Also, the system tends to a thermodynamically stable state with a uniform chemical composition, so the equilibration of a chemical potential across the sample is an additional driving force to dilute the phases with a higher In_2O_3 content towards the formation of the

equilibrium homologous phase $(\text{ZnO})_k\text{In}_2\text{O}_3$ for the starting value of k . Hence, in the Z11I sample the grains of the $(\text{ZnO})_5\text{In}_2\text{O}_3$ and $(\text{ZnO})_7\text{In}_2\text{O}_3$ phases preferentially grow at the expense of the phases with $k > 11$ until they consume them completely and all the grains have the composition of the equilibrium homologous phase $\text{Zn}_{11}\text{In}_2\text{O}_{14}$. Consequently, such grain growth results in the microstructure of the Z11I sample with large and thick plate-like grains. The samples Z5I 50-50 and Z11I 50-50 prepared from fresh and pre-reacted powders, respectively, have larger grains than the Z5I and slightly smaller than the Z11I from a fresh powder mixture. In these samples, much larger pre-reacted plate-like grains with the composition $(\text{ZnO})_k\text{In}_2\text{O}_3$ ($k=5,7,>11$) grow preferentially in accordance with Ostwald ripening at the expense of the much finer ZnO and In_2O_3 . However, the share of pre-reacted powder equal to 50% in the starting mixture of the samples Z5I 50-50 and Z11I 50-50 is likely to be too high for the development of their microstructures with even larger grains. Also, no texturing was observed in these samples, which could be expected from a spontaneous alignment of the plate-like grains in the starting mixtures during uniaxial pressing in a direction perpendicular to the pressing direction, and their preferential growth during sintering in accordance with the templated grain-growth mechanism (TGG).[22] In the case that the plate-like grains are separated

from each other, some alignment could take place for such a large addition of plate-like grains during the pressing and this would result in at least some limited amount of texturing. However, in our pre-reacted powders the plate-like grains grew together into clusters with the grains oriented in all directions (Fig. 2) and such clusters were not broken apart into separate plate-like grains during grinding in the agate mortar, which prevented any alignment during the pressing of the pellets and in the process of sintering promoted the random growth of the gains in all directions. The random growth of plate-like grains in all directions inevitably leads to empty spaces between the grains and reduces the density of the ceramics. The densities of the samples are given in Table 1.

Table 1 - Densities of the samples sintered at 1500 °C for 2 hours.

Sample	Density (g/cm ³)	Theoretical density-TD, (g/cm ³)	TD (%)
Z5I-fresh	5.58	6.12	91.2
Z5I 50:50	5.30	6.12	86.6
Z11I-fresh	5.78	5.97	96.8
Z11I 50:50	5.19	5.97	86.9

The more expressed plate-like morphology of the grains in the sample Z5I results in it having a lower density in comparison to the sample Z11I, both prepared from the fresh powder mixtures of ZnO and In₂O₃. The lower density of the samples

prepared from powder mixtures containing pre-reacted powder (ZkI 50-50) is likely the result of the already lower density of the green pellets caused by the presence of rough clusters of plate-like grains in the powder mixture and also their preferential growth during sintering.

The thermoelectric characteristics of the samples sintered at 1500 °C are graphically presented in Fig. 4. The sample Z5I prepared from the fresh powder mixture showed the highest electrical conductivity and a slightly metallic behavior; its conductivity decreased from about 310 S/cm at 100 °C to about 240S/cm at 700 °C. The sample Z5I 50-50 prepared with the addition of the pre-reacted powder had, across the whole temperature range, an approximately 40S/cm lower conductivity. The samples Y11I and Y11I 50-50 already had a significantly lower electrical conductivity, in the range from 133S/cm to 110S/cm, and from about 100S/cm to 75S/cm, respectively. The much higher electrical conductivity of the samples with the composition k=5 in comparison to the samples with k=11 could be attributed to the noticeably higher density of the InO₂⁻ planar defects, representing highly conductive paths in the homologous phase Zn₅In₂O₈ in the Zn₁₁In₂O₁₄ phase. The samples ZkI 50-50 had a similarly lower electrical conductivity in comparison to the samples ZkI with the same composition, which could be a consequence of their lower density and hence the likely weaker contacts between the grains.

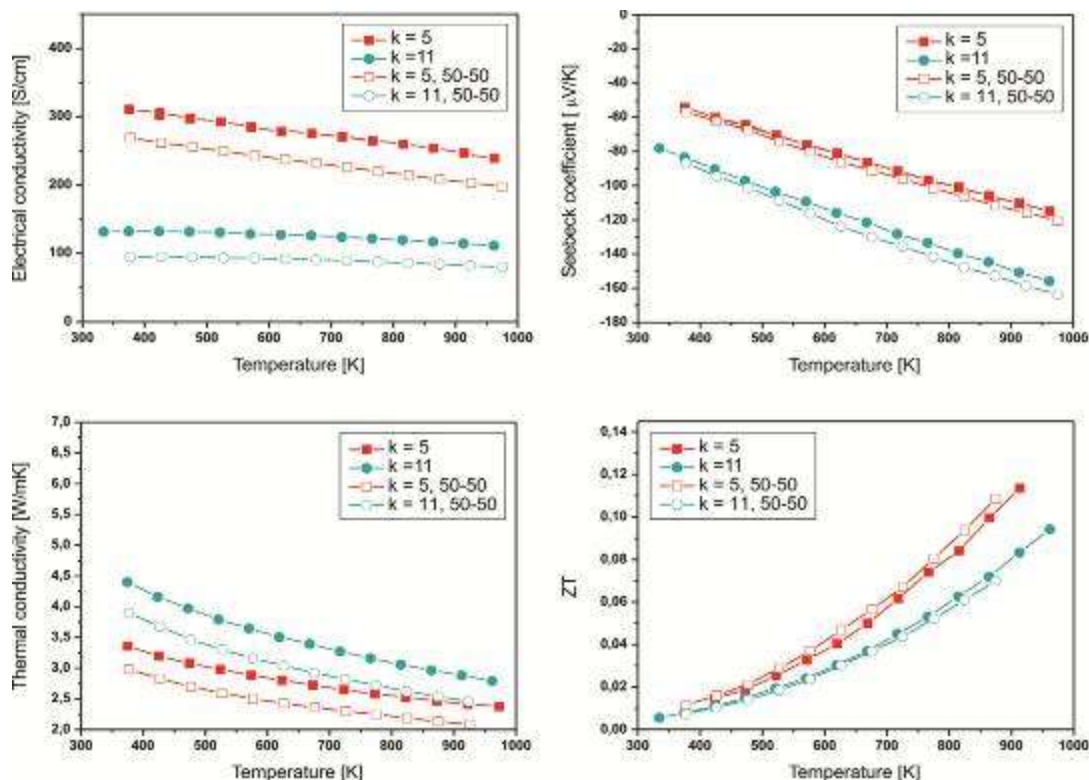


Figure 4 - Thermoelectric characteristics of the samples sintered at 1500 °C for 2 hours.

Unfortunately, the higher electrical conductivity in the case of the $(\text{ZnO})_k\text{In}_2\text{O}_3$ -based ceramics usually results in a lower Seebeck voltage (S): the samples with the composition $(\text{ZnO})_5\text{In}_2\text{O}_3$ had S in the range $-55\mu\text{V/K}$ to $-110\mu\text{V/K}$ and the samples with the composition $(\text{ZnO})_{11}\text{In}_2\text{O}_3$ were $-80\mu\text{V/K}$ to $-155\mu\text{V/K}$. The larger content of multiple planar defects caused by the In_2O_3 confirmed the benefit of a lower thermal conductivity also in this study: the samples composed of the $\text{Zn}_5\text{In}_2\text{O}_8$ homologous phase had a lower thermal conductivity than the samples of the $\text{Zn}_{11}\text{In}_2\text{O}_{11}$ phase. However, the influence of the density also clearly showed: the samples with a lower density had an approximately 0.5W/mK lower thermal conductivity than the samples with the same composition and a higher density. The ZT value for the samples with composition for $k=5$ was about 0.11 at 627°C , and this is in agreement with other reports in the literature for the $(\text{ZnO})_5\text{In}_2\text{O}_3$ homologous phase. The samples with the composition $k=11$ had a ZT of approximately 0.08, which is quite a promising result considering the much lower amount of In_2O_3 in these samples.

4. CONCLUSION

The thermoelectric $(\text{ZnO})_k\text{In}_2\text{O}_3$ -based ceramics for $k=5$ and $k=11$ were prepared using a classic ceramics procedure and sintering at 1500°C . For their preparation a fresh powder mixture of ZnO and In_2O_3 was used, or a mixture of ZnO and In_2O_3 to which pre-reacted powder with well-defined plate-like grains of the $(\text{ZnO})_k\text{In}_2\text{O}_3$ homologous phase was added to induce possible microstructure texturing in accordance with the templated grain-growth mechanism. In the case of a fresh mixture of ZnO and In_2O_3 the process of phase formation is controlled by the uniformity of the distribution of the In_2O_3 powder in the matrix of ZnO powder, which determines the local concentration of In_2O_3 and hence the local ZnO-to- In_2O_3 ratio in the mixture. In compositions with larger additions of In_2O_3 than $k=5$ it is present in sufficient amounts everywhere in the mixture for basically the direct formation of the $\text{Zn}_5\text{In}_2\text{O}_8$ homologous phase. In compositions with a much smaller addition of In_2O_3 than for $k=11$ it is locally either in excess, which results in the formation of the $\text{Zn}_5\text{In}_2\text{O}_8$ and $\text{Zn}_7\text{In}_2\text{O}_{10}$ phases, or in deficit, so that the $(\text{ZnO})_k\text{In}_2\text{O}_3$ phases for $k>11$ towards the pure ZnO are formed. With further processing the grains of the $\text{Zn}_5\text{In}_2\text{O}_8$ and $\text{Zn}_7\text{In}_2\text{O}_{10}$ phases grow at the expense of the high- k $(\text{ZnO})_k\text{In}_2\text{O}_3$ phases, which leads to the formation of the equilibrium $\text{Zn}_{11}\text{In}_2\text{O}_{14}$ phase. When the starting-powder mixture contains pre-reacted powder with much coarser, plate-like grains of the $(\text{ZnO})_k\text{In}_2\text{O}_3$ homologous phases, the low- k phases ($\text{Zn}_5\text{In}_2\text{O}_8$

and $\text{Zn}_7\text{In}_2\text{O}_{10}$) grow at the expense of the much finer grains of ZnO and In_2O_3 , and also the high- k $(\text{ZnO})_k\text{In}_2\text{O}_3$ homologous phases, which finally results in the formation of the equilibrium $(\text{ZnO})_k\text{In}_2\text{O}_3$ homologous phase for the starting k value in the whole sample. Nevertheless, the final microstructures of all the samples, regardless of the starting mixture, were similar. No texturing was observed in the samples prepared from the starting mixtures containing pre-reacted plate-like grains of the $(\text{ZnO})_k\text{In}_2\text{O}_3$ homologous phases. However, these samples had a lower density, likely the result of a lower density of green pellets caused by the presence of solid clusters of plate-like grains together with fine powders of ZnO and In_2O_3 in the starting mixture.

The TE characteristics of the samples $(\text{ZnO})_k\text{In}_2\text{O}_3$ are in general influenced by the starting composition for the k value. The results showed no significant influence of the starting-powder mixture on the ZT values and were similar for the samples with the same composition of k . The samples with $k=5$, as expected, showed a higher ZT of 0.11 at 627°C in comparison to the 0.08 for the compositions with $k=11$. However, considering the much smaller amount of In_2O_3 in the sample with $k=11$ the obtained result seems promising.

Acknowledgements

This work was supported by the Slovenian Research Agency (Young Researcher Program PR-04363, Project Grant L2-4192 and Program Contact Number P2-0084) and the Slovene Human Resources Development and Scholarship Fund (Contract No. 11012-12/2013).

5. REFERENCES

- [1] H.J.Goldsmid (2010) Introduction to thermoelectricity, Springer, London
- [2] X.Zhang, L.D.Zhao (2015) Thermoelectric materials: energy conversion between heat and electricity, Journal of Materiomics, 1, 92-105
- [3] X.F.Zheng, C.X.Liu, Y.Y.Yan, Q.Wang (2014) A review of thermoelectrics research – recent development and potentials for sustainable and renewable energy applications, Renewable and Sustainable Energy Reviews, 32, 486-503.
- [4] J.Yang, Thierry Caillat (2006) Thermoelectric Materials for Space and Automotive Power Generation, MRS Bulletin, 31, 224-229.
- [5] S.Sano, H.Mizukami, H.Kaibe (2003) Development of high-efficiency thermoelectric power generation system, Komay'su Technical Report, 49(152), 1-7.
- [6] J.F.Li, W.S.Liu, L.D.Zhao, M.Zhou (2010) High-performance nanostructured thermoelectric materials, NPG Asia Materials, 2(4), 152-158.
- [7] G.J.Snyder, E.S.Toberer (2008) Complex thermoelectric materials, Nature, 7, 105-114.

- [8] S.Walia, S.Balendhran, H.Nili, S.Zhuykov, G.Rosengarten, Q.H.Wang, M.Bhasharan, S.Sriram, M.S.Strano, K.Kalantar-zadrh (2013) Transition metal oxides – thermoelectric properties, *Progress in Materials Science*, 58, 1443-1489.
- [9] J.W.Fergus (2012) Oxide materials for high temperature thermoelectric energy conversion, *Journal of the European Ceramic Society*, 32, 525-540.
- [10] J.He, Y.Liu, R.Funahashi (2011) Oxide thermoelectrics: the challenges, progress, and outlook, *Journal of Materials Research*, 26(15), 1762-1772.
- [11] I.Terasaki, Y.Sasago, K.Uchinokura (1997) Large thermoelectric power in NaCo_2O_4 single crystal, *Physical Review B*, 56, 12685-12687.
- [12] M. Presecnik, J.de Boor, S.Bernik (2016) Synthesis of single-phase $\text{Ca}_3\text{Co}_4\text{O}_9$ ceramics and their processing for a microstructure-enhanced thermoelectric performance, *Ceramics International*, 42, 7315-7327.
- [13] M.Ohtaki, T.Tsubota, K.Eguchi, H.Arai (1996) High-temperature thermoelectric properties of $\text{Zn}_{(1-x)}\text{Al}_{(x)}\text{O}$, *Journal of Applied Physics*, 79, 1816-1818.
- [14] M. Ohtaki, K. Araki, K. Yamamoto (2009) High Thermoelectric Performance of Dually Doped ZnO Ceramics, *Journal of Electronic Materials*, 38, 1234-1238.
- [15] T. Moriga, D.D. Edwards, T.O.Mason, G. B. Palmer, K. R. Poeppelmeier, J.L.Schindler, C.R.Kannewurf, I.Nakabayashi (1998) Phase Relationships and Physical Properties of Homologous Compounds in the Zinc Oxide-Indium Oxide System, *Journal of the American Ceramics Society*, 81, 1310-1316.
- [16] H.Ohta, W.S. Seo, K. Koumoto (1996) Thermoelectric Properties of Homologous Compounds in the $\text{ZnO-In}_2\text{O}_3$ System, *Journal of the American Ceramic Society*, 79, 2193-2196.
- [17] L.M.Wang, C.Y.Chang, S.T.Yeh, S.W.Chen, Z.A.Peng, S.C.Bair, D.S.Lee, F.C.Liao, Y.K.Kuo (2012) Synthesis and post-annealing effects on the transport properties of thermoelectric oxide $(\text{ZnO})_m\text{In}_2\text{O}_3$ ceramics, *Ceramics International*, 38, 1167-1174.
- [18] X.Liang, D.R.Clarke (2014) Relation between thermoelectric properties and phase equilibria in the $\text{ZnO-In}_2\text{O}_3$ binary system, *Acta Materialia*, 63, 191-201.
- [19] A.Rečnik, N.Daneu, S.Bernik (2007) Nucleation and growth of basal-plane inversion boundaries in ZnO, *Journal of the European Ceramic Society*, 27, 1999-2008.
- [20] T.Tani, S.Isobe, W.S. Seo, K.Koumoto (2001) Thermoelectric properties of highly textured $(\text{ZnO})_5\text{In}_2\text{O}_3$ ceramics, *Journal of Materials Chemistry*, 11, 2324-2328.
- [21] D.F.Anthrop, A.W.Searcy (1964) Sublimation and Thermodynamic Properties of Zinc Oxide, *The Journal of Physical Chemistry*, 68, 2335-2342.
- [22] E.Suvaci, G.L. Messing (2000) Critical Factors in the Templated Grain Growth of Textured Reaction-Bonded Alumina, 83(8), 2041-2048.

IZVOD

MIKRO-STRUKTURNE I TERMO-ELEKTRIČNE KARAKTERISTIKE KERAMIKE NA BAZI $(\text{ZnO})_k\text{In}_2\text{O}_3$ (K = 5 I 11)

Visoko-temperaturna keramika na bazi oksida je neophodna za primenu u visoko-temperaturnim aplikacijama koje uključuju sakupljanje otpadne toplote direktnom transformacijom u električnu energiju. U slučaju n-tipa materijala, odgovarajuće faze tipa $(\text{ZnO})_k\text{In}_2\text{O}_3$ veoma su pogodne za obezbeđivanje određenih termo-električnih (TE) svojstava. U ovom radu formirane su TE keramike na bazi $(\text{ZnO})_k\text{In}_2\text{O}_3$ za $k=5$ i 11 klasičnim keramičkim postupkom i sinterovannjem na $1500\text{ }^\circ\text{C}$. U toku njihove pripreme korišćeni su ili smeše sveže pripremljenih prahova ZnO i In_2O_3 , ili smeše ZnO i In_2O_3 koje su sadržale pločasta zrna već proreagovane $(\text{ZnO})_k\text{In}_2\text{O}_3$ faze, da bi se izazvala moguća tekstura materijala. Pokazano je da početni sastav u smislu k vrednosti, kao i tip polaznih prahova, utiču na proces dovodeći do formiranja ravnotežne $(\text{ZnO})_k\text{In}_2\text{O}_3$ faze, kao i do formiranja određene mikro-strukture. Pored toga, svi uzorci su imali sličnu konačnu mikro-strukturu i nije primećena nikakva tekstura uzoraka. Bez obzira na upotrebu različitih polaznih smeša prahova, uzorci sa istim sastavom su posedovali slične vrednosti bezdimenzionog faktora ZT (koji karakteriše TE osobine materijala): na $627\text{ }^\circ\text{C}$ ZT je bilo 0.11 za uzorke sa $k = 5$ i 0.08 za $k = 11$, što nije zanemarljivo ako se uzme u obzir znatno manji sadržaj In_2O_3 u uzorcima sa $k = 11$.

Ključne reči: ZnO keramika, dopovanje sa In_2O_3 , mikro-struktura, termo-električne osobine.

Naučni rad

Rad primljen: 09. 03. 2016.

Rad prihvaćen: 14. 04. 2016.

Rad je dostupan na sajtu: www.idk.org.rs/casopis